LAWRENCE
LIVERMORE
NATIONAL
LABORATORY

LLNL-TR-411072

A Predictive Model of Fragmentation using Adaptive Mesh Refinement and a Hierarchical Material Model

A. E. Koniges, N. D. Masters, A. C. Fisher, R. W. Anderson, D. C. Eder, D. Benson, T. B. Kaiser, B. T. Gunney, P. Wang, B. R. Maddox, J. F. Hansen, D. H. Kalantar, P. Dixit, H. Jarmakani, M. A. Meyers

March 5, 2009

Disclaimer

This document was prepared as an account of work sponsored by an agency of the United States government. Neither the United States government nor Lawrence Livermore National Security, LLC, nor any of their employees makes any warranty, expressed or implied, or assumes any legal liability or responsibility for the accuracy, completeness, or usefulness of any information, apparatus, product, or process disclosed, or represents that its use would not infringe privately owned rights. Reference herein to any specific commercial product, process, or service by trade name, trademark, manufacturer, or otherwise does not necessarily constitute or imply its endorsement, recommendation, or favoring by the United States government or Lawrence Livermore National Security, LLC. The views and opinions of authors expressed herein do not necessarily state or reflect those of the United States government or Lawrence Livermore National Security, LLC, and shall not be used for advertising or product endorsement purposes.

Auspices Statement

This work performed under the auspices of the U.S. Department of Energy by Lawrence Livermore National Laboratory under Contract DE-AC52-07NA27344. This work was funded by the Laboratory Directed Research and Development Program at LLNL under project tracking code 06-ERD-036.

FY08 LDRD Final Report
A Predictive Model of Fragmentation using Adaptive Mesh Refinement and a Hierarchical Material Model
DRD Project Tracking Code: 06-ERD-036

Alice Koniges, Principal Investigator

Abstract

Fragmentation is a fundamental material process that naturally spans spatial scales from microscopic to macroscopic. We developed a mathematical framework using an innovative combination of hierarchical material modeling (HMM) and adaptive mesh refinement (AMR) to connect the continuum to microstructural regimes. This framework has been implemented in a new multi-physics, multi-scale, 3D simulation code, NIF ALE-AMR. New multi-material volume fraction and interface reconstruction algorithms were developed for this new code, which is leading the world effort in hydrodynamic simulations that combine AMR with ALE (Arbitrary Lagrangian-Eulerian) techniques. The interface reconstruction algorithm is also used to produce fragments following material failure. In general, the material strength and failure models have history vector components that must be advected along with other properties of the mesh during remap stage of the ALE hydrodynamics. The fragmentation models are validated against an electromagnetically driven expanding ring experiment and dedicated laser-based fragmentation experiments conducted at the Jupiter Laser Facility. As part of the exit plan, the NIF ALE-AMR code was applied to a number of fragmentation problems of interest to the National Ignition Facility (NIF). One example shows the added benefit of multi-material ALE-AMR that relaxes the requirement that material boundaries must be along mesh boundaries.

I. Introduction/Background

Great strides have been made in numerical modeling of problems in solid mechanics in the last 20 years. For example, Lagrangian simulations of automobile crashes with millions of zones on modest computer clusters are routinely used by industry to design safer automobiles. Despite these advances, computational solid mechanics (CSM) lags in comparison to computational fluid dynamics (CFD) in many areas. While CFD simulations that are uniformly second-order accurate in both time and space are routine, and the development of higher-order-accurate algorithms is an area of intense research, multi-material Eulerian CSM simulations are still only first-order accurate at material interfaces. In addition, there are entire areas of physical phenomena in solid mechanics that are poorly understood theoretically, and reliable simulation technology is virtually nonexistent.

Fragmentation, for example, occurs at a wide range of temporal and spatial scales, from atomistic to cosmological, but the underlying phenomenology is poorly understood, and the simulation technology is primitive. Fragmentation is a phenomenon that is intrinsically multi-scale; small variations in the microstructure lead to a distribution of

localized failure sites that ultimately coalesce to form macroscopic fragments. [1-3] Virtually all fragmentation experiments also show an overall particle distribution that is exponential in nature.

Historically, hydrodynamic simulations have used ALE or AMR techniques. Our research builds on the pioneering work that combined these techniques for gas dynamic simulations. [4-8] This earlier work made use of the SAMRAI infrastructure developed for AMR simulations. [9] We continue to use SAMRAI as we add solid mechanics and other multi-physics capabilities to our new code, NIF ALE-AMR. In addition to the mapping of the standard state variables (density, energy, etc), coupling with the HMM requires the mapping of representations of material parameters, including history variables, that account for the microstructural heterogeneity at the smallest scales.

The size of NIF targets is approximately 1 cm. Typical microstructure such as grain structure is on the order of ~10 microns. This provides strong motivation for the development of AMR and HMM algorithms to span the length scales where the solutions can be verified experimentally and computationally with nearly full-resolution simulations. Modeling of ductile metals as well as brittle materials such as Si and Be are important for NIF. Metals have a microstructure composed of individual grains. The shape, size, and lattice orientation of these individual grains has a profound influence on the macroscopic mechanical properties of the material. [2,3,10] Additionally, the individual grains may have microstructure with defects or inclusions, voids, or alternate phases, all of which contribute to the mechanical response of the material. The heterogeneity of the microstructure of both ductile and brittle material means that stress within a representative volume element (RVE) is not uniform even when the material is subjected to uniform loading or deformation.

II. Research Activities

Our research includes developing a mathematical framework for material strength and failure using HMM and AMR to connect the continuum to microstructural regimes as well as implementing this framework in a new multi-physics, multi-scale, 3D simulation code, NIF ALE-AMR. The framework includes a variety of models including simple isotropic continuum models such as Johnson-Cook, and more complicated anisotropic microscale models such as single crystal plasticity. Additionally the code includes a void fracture model that allows for fragment formation. We start with a brief overview of the algorithms in NIF ALE-AMR followed by details of the multi-material volume fraction and interface reconstruction method. We conclude this section with additional information associated with adding solid mechanics to the code.

The basic algorithm in NIF ALE-AMR consists of Lagrange motion plus remap (ALE) followed by regridding/rezoning (AMR). The Lagrange step utilizes a staggered grid, i.e., velocities are nodal quantities while other quantities such as density and energy are zone centered. Remapping refers to the interpolation of nodal and zonal quantities on the current mesh to either the original (Eulerian) or relaxed (ALE) mesh configuration and is treated as an advection problem. One consequence of an ALE (or Eulerian) algorithm is that material interfaces, which are tracked naturally by a conformal Lagrangian mesh,

must be reconstructed as they are advected away from the mesh interfaces. The most prevalent methods for interface reconstruction involve storing volume fractions of the material components within mixed zones and reconstructing interfaces as needed. [11-13] In mixed zones, the contributions of the component materials to the advected material must be determined. We utilize a standard method that uses the volume fractions of neighboring zones to approximate the orientation of the material interfaces within a donor zone and then to select a likely ordering for the materials to be advected. This avoids explicitly reconstructing the interfaces during the advection step and has been shown to work well in practice. Finally, groups of zones are coarsened or refined based on various criteria to maintain accuracy and reduce computational expense (AMR).

User defined criteria are used to identify regions that may be coarsened or refined—refining the mesh to maintain accuracy in regions with rapidly changing dynamics and coarsening in less dynamic regions to reduce computational expense. In the case of clean zones, the coarsened quantities are averaged by volume or mass weighting. The same method may be used for mixed zones, with the volume fraction of the coarsened zones being the volume weighted average of the volume fractions of the fine zones being coarsened. Refinement poses a much more difficult problem. In a clean coarse zone, the zonal and nodal quantities may be interpolated to the new refined zones by defining a gradient in terms of the neighboring zones. However, we cannot utilize gradient-based interpolation for mixed zones. Furthermore, we must first determine the composition of the refined zones (clean or mixed and volume fractions). This requires an explicit reconstruction of the interface. From the stored volume fractions we again calculate the orientation of each interface and then solve for the location corresponding to the appropriate truncated volume within the coarse zone. Intersecting this reconstructed interface with the refined zones yields the necessary compositions and associated volume fractions. In 3D, the zones are general hexahedra, bounded on six sides by doubly ruled surfaces. We have developed a method, similar to that proposed by Kothe, [14] which is used to determine the volume of a general (including degenerate) hexahedron truncated by planar interfaces. This new method, which is also used for shaping of complex geometries in non-conformal meshes, not only allows for an arbitrary number and configuration of material interfaces but is faster than alternative methods, e.g., faceted representations of the zones. Once the composition of the refined zones has been determined, the zonal quantities are assigned using the constant values for the mixed quantities of the parent coarse zones. The nodal velocities again depend on the composite quantities and are interpolated in the same manner for clean and mixed zones.

The addition of solid mechanics to the code requires tracking additional quantities including the stress tensor, strain rate, and the material history vector. The material history vector is necessary to store any other persistent data that a material model requires, for instance the level of accumulated damage in models including material failure or the evolving yield stress in J2 plasticity models. In order to tie the full stress tensor into the gas-dynamics equation being solved in NIF ALE-AMR, the equation of motion is updated with an additional stress term. During the Lagrange step, additional forces acting on the nodes from stress components results in nodal accelerations and displacements. Within mixed zones the pressures and stresses are weighted by the

volume fractions of the component materials to obtain composite quantities. Mesh deformations are used to determine volumetric and deviatoric strain rates, which must be partitioned amongst component materials in mixed zones, often altering the volume fractions. In NIF ALE-AMR strains rates are partitioned based on the material volume fractions and the bulk moduli for volumetric component or the shear moduli for deviatoric components. The strain rates and the current stress and material state (plastic strain, damage, etc.) for each material (in clean or mixed zones) are then used to update the internal energy and the stress state—including hardening and failure—based on appropriate material models, e.g., the Johnson-Cook model. [15]

If failure is detected a special void material is inserted. If the material fails in tension a volume fraction of void is introduced to take up the volume gained in the current time step. If the cell fails in compression a small volume fraction (10^{-6}) of void material is inserted into the cell. As cells continue to deform the fraction of void materials in failed cells will change to take up subsequent changes in volume. As failures occur in neighboring cells the interface reconstruction algorithm allows the voids to coalesce and form void regions. Finally as these regions spread through the body of the object fragmentation occurs. This is shown in Figure [1]. The effect of void insertion and subsequent fragmentation is demonstrated in the simulation results presented in the next section.

As part of the algorithmic research for this LDRD, we are developing a laser input package to model laser energy deposition in the experiments. We are also incorporating a diffusion and conduction model into the material/hydro simulation.

III. Results/Technical Outcome

The fragmentation of expanding rings is a problem of particular interest to NIF where target assemblies can include rings on the outside of the hohlraum as a bridge to a cryogenic cooling apparatus. During a NIF shot the hohlraum is expected to vaporize and rapidly expand outward, pushing the cooling rings with it. This expansion will cause the ring to fragment in a number of pieces with sizes and velocities that are of great interest to the NIF program. There is very little available experimental data involving hohlraum driven ring expansion. However, there are papers providing fragmentation data for electromagnetically driven rings that can be used for code validation. [16] A schematic for an electromagnetically driven expanding ring experiment is shown in Figure [2]. The energy discharged into the solenoid from the capacitor induces a current in the ring causing it to heat and expand outward. In the experiment we chose to model, 1-mm thick Al rings with inner and outer diameters of 30.5 mm and 32.5 mm were placed around a solenoid. A capacitor bank was then charged to one of a variety of voltages and used to discharge 0.94 kJ – 3.12 kJ of energy through the solenoid. The current flowing through the solenoid produces a large magnetic field, which in turn induces a current in the ring. This induced current has two effects. The first is resistive heating of the ring. The second is a magnetic field that results in a repulsive force between the solenoid and the ring, causing the ring to expand outward. By varying the voltage to which the capacitor is charged, a range of velocities and temperatures were studied. They tracked the maximum expansion velocities (50 m/s – 300 m/s) and the temperature rises in the ring experiments

(110 K – 240 K). Finally, after each ring was accelerated, the fragments were collected, counted, and analyzed. The resulting fragment counts were compared with previous theoretical work relating the number of fragments to the total kinetic energy. In Figure [3] we see that fragmentation predictions using NIF ALE-AMR are in good agreement with the data.

We have also benchmarked NIF ALE-AMR with LS-DYNA, which is a private sector finite element code capable of structural failure modeling in the Lagrangian frame. It is used extensively in applications with a need for high reliability such as automobile crash-worthiness and earthquake safety engineering of bridges. While LS-DYNA is missing many of the critical features in NIF ALE-AMR, it has been through a great deal of quality assurance testing, and thus is an excellent code with which to compare results. Another ring fragmentation problem was chosen for this code-to-code comparison. A quarter of the ring was discretized with 30 elements across the radius and 150 elements around the 90-degree wedge. The material model used for the rings was again Johnson-Cook for Al 6061-T6, including a ±5% random seeding of the D_2 parameter. A pressure load of 0.003 Mbar was applied to the inner surface of the ring in the LS-DYNA simulation. Similarly extra elements filled with pressurized void on the inside of the ring provided the load in the NIF ALE-AMR simulation. It should be noted that the fracture model in LS-DYNA is far simpler than the NIF ALE-AMR algorithm described previously. Upon failure in LS-DYNA a cell is removed from the mesh and the simulation continues without it. For the purpose of this comparison, the NIF ALE-AMR fracture model was altered to mimic this behavior. Instead of introducing a small amount of void upon failure, the material in the cell is replaced with void—mimicking the removal of the cell. This allowed for better comparisons between LS-DYNA and NIF ALE-AMR. Both simulations were allowed to run in pure Lagrange time steps for 15μs and the results are compared Figure 4. The results of this comparison are quite good. Both rings are showing similar levels of accumulated plastic strain and are breaking into similar sized fragments

To provide data for additional validation of the code, we conducted experiments at the Janus laser, which is part of the Jupiter Laser Facility at LLNL. During these experiments, thin metal, e.g., Vanadium, foils were heated by a laser resulting in front-surface ablation and rear-surface spall. The spalled fragments were captured either on glass plates (Figure [5]) or in aerogel foam (Figure [6]). The aerogels were radiographed to obtain the size, depth, and spatial distribution of the fragments. This information was used to determine the velocity of the fragments using a simple snowplow-stopping model [18]. The 2D NIF ALE-AMR simulation of a Vanadium foil presented in Figure [7] illustrates the codes ability to model fragmentation. Comparison of the experimental data with more detailed simulations is on-going.

As part of our exit plan, we decided to demonstrate the capability of NIF ALE-AMR on the fragmentation of the cooling rings surrounding a hohlraum. The current NIF design used Si cooling rings while the French are considering Al cooling rings. We have modeled Si and Al rings for the same loading using brittle and ductile strength/failure models, respectively. The result for Si at 1.45 microseconds is shown in Figure [8]. We

calculate that Si breaks into small relatively fast moving fragments. In contrast, the result for an Al ring at 14 microseconds is shown in Figure [9], where the fragments are larger and slower moving. Based on experiments and modeling, it appears that the Si fragments are less likely to damage NIF optics than Al fragments.

As an additional demonstration of NIF ALE-AMR capability, we modeled a NIF target that is part of the shock timing campaign on the path to demonstrate fusion in the laboratory. This target consists of a hohlraum with a cone that penetrates the side of the hohlraum as well as the capsule that is inside. By looking down the inside of the cone, one can observe shocks breaking out on the inside of the capsule. During the design of this experiment, there was concern that the outer portion of the cone could be launched with significant velocity and damage a diagnostic. When this complex target was modeled we benefited from the multi-material capability of ALE-AMR that relaxes the requirement for conformal meshes, i.e., that material boundaries must be along mesh boundaries. The AMR nature of the code allows for additional refinement at material boundaries. The results of the simulation are shown in Figure [10]. We calculate that the velocity of the outer cone is acceptable.

The HMM allows fine-scale modeling of the initial fragmentation using a range of models including computationally expensive crystal plasticity, while the elements at the mesoscale can use a simpler models such as polycrystal models, and the macroscopic elements use analytical flow stress models. We have demonstrated that the code can calculate material properties using these different models one at a time. Additional work is required to achieve the final goal of using different models at the same time on different levels of refinement with corresponding communication between the levels.

IV. Exit Plan

This project is on the forefront of computational research in a major thrust area based on multi-scale simulations. By using the CASC-developed SAMRAI (structured AMR) framework as our application base for the NIF ALE-AMR research, we have positioned SAMRAI to be a major player in these new multi-physics simulations. The fragmentation model developed under this proposal and its implementation in NIF ALE-AMR is being used actively for debris and shrapnel assessments on all targets to be shot on NIF. Both post-doctoral researchers hired as part of this proposal are in the NIF plans to be funded at 100% level out to at least FY12 as they transition to staff positions during this period. Collaborators in the US currently have access to the code, which allows them to independently set-up problems relevant to use of NIF as a user facility. In addition, the French government has formally requested permission to use NIF ALE-AMR for debris and shrapnel simulation for their Laser MegaJoule (LMJ) facility. Discussions are ongoing with the Export Control office to allow for this important exchange. Our research also gives CASC and NIF researchers an additional tool on which to build collaborations and seek new funding opportunities. For example, our joint proposal with UCLA, “Multiscale Methods for Fracture and Multimaterial Debris Flow,” for UC LAB management funding was ranked 2nd out of 135 in the category of Engineering, Computer Science, Math and Statistics with funding of $500k/year awarded. In addition, we submitted two proposals to the OFES-NNSA Joint Program on HEDLP, “Modeling Ion-

Heated Warm Dense Matter experiments with the Full Stress Tensor, Material History, and Phase Transitions," in collaboration with LBL and "Hydro-Coupled Laser Plasma Interactions with Hierarchical Physics Models."

V. Summary

This research has significantly advanced the field in multi-physics, multi-scale 3D simulations. We have developed a mathematical framework for material strength and failure using HMM and AMR, which connects the continuum to microstructural regimes, and implemented this framework in a new simulation code, NIF ALE-AMR. As a result of this LDRD, NIF has a significantly improved capability to predict fragmentation and dismantling of target components fielded as part of the overall ignition plan do demonstrate inertial fusion in the laboratory. We developed a predictive capability for fragmentation on a numerical simulation level rather than with traditional heuristic models. This capability reduces the risk to NIF optics and diagnostics from damage due to target shrapnel. Additional value for NIF is in the understanding of fragmentation and target ejecta process in order to contain special materials, e.g., Beryllium filters. New collaborations that make use of this research are being explored as well. This research resulted in six refereed publications [19-24], two invited talks at international conferences, and four additional publications in progress [25-28].

VI. Acknowledgements

Laser spall experiments were conducted at the Jupiter Laser Facility at LLNL. We gratefully acknowledge both the time granted for these experiments and the assistance of Dwight Price and other Jupiter Laser Facility personnel. We appreciate insight and help provided by Rich Becker and Nathan Barton on material models.

VII. References

[1] D. E. Grady, "Local Inertial Effects in Dynamic Fragmentation," *J. Appl. Phys.* 53(1), 322-325 (1981).
[2] R. Becker, O. A. Hurricane, H. K. Springer, and A. Sunwoo, "Material Models for Fragmentation of Ductile Metals," UCRL-PRES-155072, (2003).
[3] R. Becker, "Ring Fragmentation Predictions Using the Gurson Model with Material Stability Conditions as Failure Criteria," *International Journal of Solids and Structures,* 39, 3555-3580, (2002).
[4] J. Bell, M. Berger, J. Saltzman, M. Welcome, "Three dimensional adaptive mesh refinement for hyperbolic conservation laws," *SIAM Journal on Scientific Computing*, 15, 127-138, (1994).
[5] M. Berger, J. Oliger, "Adaptive mesh refinement for hyperbolic partial differential equations," *Journal of Computational Physics*, 53, 484–512, (1984).
[6] M. Berger, P. Colella, "Local adaptive mesh refinement for shock hydrodynamics," *Journal of Computational Physics*, 82, 64–84, (1989).
[7] R. Pember, J. Bell, P. Colella, W. Crutchfield, M.L. Welcome, "An adaptive Cartesian grid method for unsteady compressible flow in complex geometries," *Journal of Computational Physics*, 120, 278–304, (1995).

[8] J. Bell, P. Colella, J. Trangenstein, M. Welcome, “Adaptive mesh refinement on moving quadrilateral grids,” in: *Proceedings, AIAA 9th Computational Fluid Dynamics Conference*, Buffalo, New York, June 14–16, 471–579, (1989).
[9] R.W Anderson, N.S. Elliott, R.B. Pember, “An arbirtrary Lagrangian-Eulerian method with adaptive mesh refinement for the solution of the Euler Equations,” *Journal of Computational Physics*, 199 (2), 598-617, (2004).
[10] R. J. Asaro, “Overview No. 42, Texture Development and Strain Hardening in Rate Dependent Polycrystals,” *Acta metall,* (33)6, 923-953 (1985).
[11] C.W. Hirt and B.D. Nichols, “Volume of fluid (VOF) method for the dynamics of free boundaries,” *Journal of Computational Physics*, 39, 201–225, (1981).
[12] D. J. Benson, “Volume of fluid interface reconstruction methods for multi-material problems,” *Applied Mechanics Review*, 55, 151–165, (2002).
[13] A. Stagg, R. Boss, J. Grove, and N. Morgan, “Interface modeling: A survey of methods with recommendations,” *Technical Report LA-UR-05-8157*, Los Alamos National Laboratory, (2005).
[14] D.B. Kothe, M.W. Williams, K.L. Lam, D.R. Korzekwa, P.K. Tubesing, E.G. Puckett, “A second-order accurate, linearity-preserving volume tracking algorithm for free surface flows on 3-D unstructured meshes,” in: *Proceedings of the 3rd ASME/JSME Joint Fluids Engineering Conference*, San Francisco, California, July 18-22, (1999).
[15] G. Johnson, W. Cook, “Fracture characteristics of three metals subjected to various strains, strain rates, temperatures, and pressures,” *Engineering Fracture Mechanics*, 21 (1985) (1).
[17] Altanova M, Hu X., Daehn G., “Increased ductility in high velocity electromagnetic ring expansion,” *Metallurgical and Materials Transactions* A 27 (1996)
[18] M. Tobin, J. Andrew, D. Haupt, K. Mann. J. Poco, J.Satcher, D. Curran, R. Tokheim, and D. Eder, “Using Silica Aerogel to Characterize Hypervelocity Shrapnel Produced in High Power Laser Experiments,” *International Journal of Impact Engineering*, 29, 713-721, (2003).
[19] A. E. Koniges, B. T.N. Gunney, R. W. Anderson, A. C. Fisher, N. D. Masters. "Development Strategies for Modern Predictive Simulation Codes", *Advances in Parallel Computing*, 15, 697-704, (2008).
[20] N.D. Masters, R.W. Anderson, N.S. Elliott, A.C. Fisher, B.T. Gunney and A.E. Koniges. "Interface reconstruction in two- and three-dimensional arbitrary Lagrangian-Eulerian adaptive mesh refinement simulations", *Journal of Physics: Conference Series*, 112 (2008) 022017.
[21] A. C. Fisher N. D. Masters A. E. Koniges R. W. Anderson B. T. N. Gunney P. Wang R. Becker D. J. Benson P. Dixit. "Hieraechical Material Models for Fragmentation Modeling in NIF-ALE-AMR", *Journal of Physics: Conference Series*, 112 (2008) 022027.
[22] D. Eder A. Koniges O. Landen N. Masters A. Fisher O. Jones T. Suratwala L. Suter. "Debris and Shrapnel Mitigation Procedure for NIF Experiments", *Journal of Physics: Conference Series*, 112 (2008) 032023.
[23] A. Koniges C. Debonnel J. Andrew D. Eder D. Kalantar N. Masters A. Fisher R. Anderson A. Gielle B. Gunney K. Sain J. Jadaud A. Tobin N. Meyers H. Jarmakani. "Experiments for the validation of debris and shrapnel calculations", *Journal of Physics: Conference Series*, 112 (2008) 032072.

[24] D. Benson P. Dixit A. E. Koniges A. C. Fisher N. D. Masters R. W. Anderson B. T. Gunney D. C. Eder. "Hierarchical Material Models for Modeling Fragmentation of Targets in Inertial Confinement Fusion Research", in: *Proceedings of the International Symposium on Structures under Earthquake, Impact, and Blast Loading*, Osaka, Japan, Nov 10-11, (2008).
[25] A. Fisher, D. Benson, A. Koniges, D. Eder, N. Masters, R. Anderson, "Validation for fragmentation modeling in NIF ALE-AMR," in progress.
[26] A. Fisher, D. Bailey, B. Gunney, A. Koniges, D. Eder, N. Masters, R. Anderson, "Heat conduction and radiation transport modeling in NIF ALE-AMR," in progress.
[27] N.D. Masters, R.W. Anderson, B.T.N. Gunney, A. Fisher, A.E. Koniges, "An analytic and efficient solution to the partial volume of truncated hexahedral zones," in progress.
[28] N.D. Masters, T. Kaiser, R.W. Anderson, A. Fisher, A.E. Koniges, "Laser raytracing in a parallel adaptive mesh refinement hydrocode," in progress.

VII. Figures

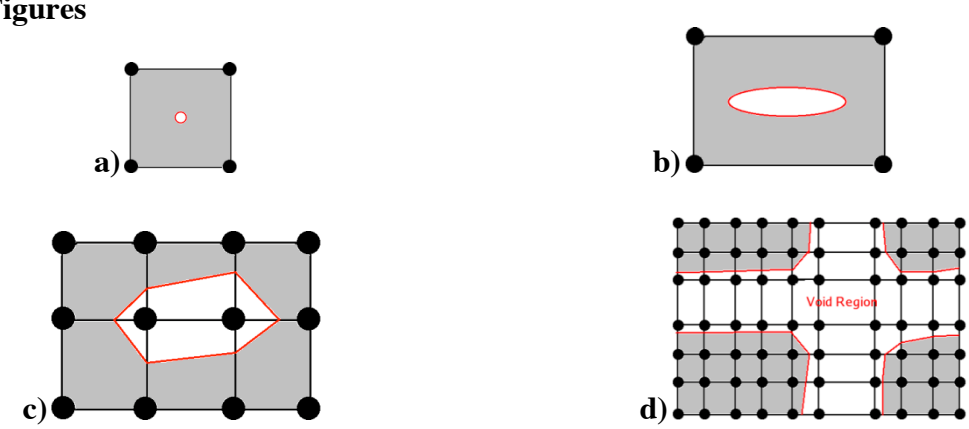

Figure 1: Fracture and fragmentation approach in NIF ALE-AMR. a) Upon material failure a small volume of void is inserted. b) As the cell expands in subsequent time steps, the void grows. c) As neighboring cells accumulate void, the interface reconstruction algorithms allow the voids to coalesce and form crack regions. d) Crack regions can grow large enough to span entire cells allowing fragments to form and detach from the material body.

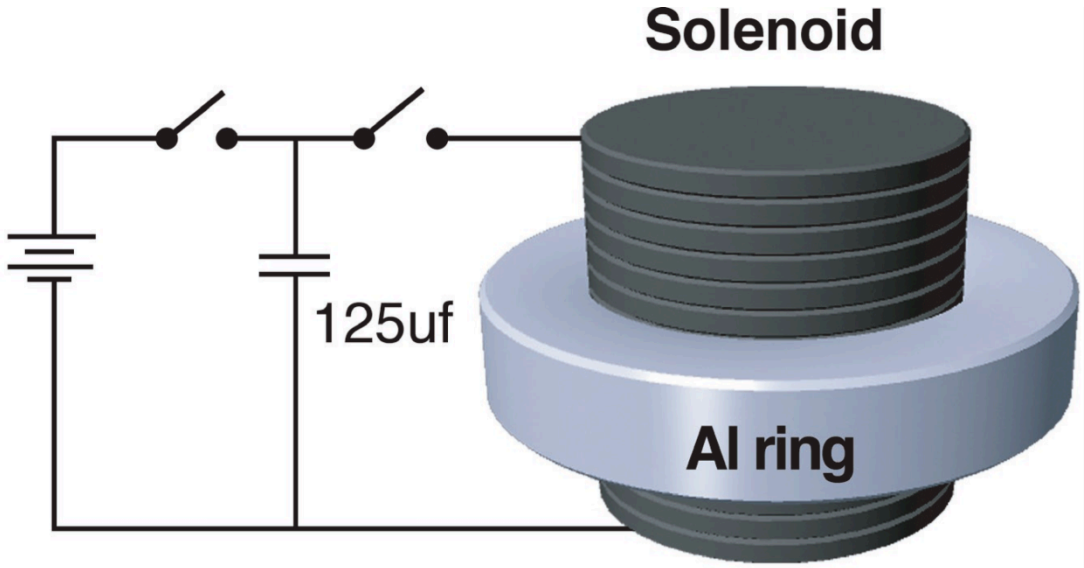

Figure 2: Schematic for the electromagnetically driven expanding ring experiments. The energy discharged into the solenoid induces a current in the ring which causes heating and outward expansion.

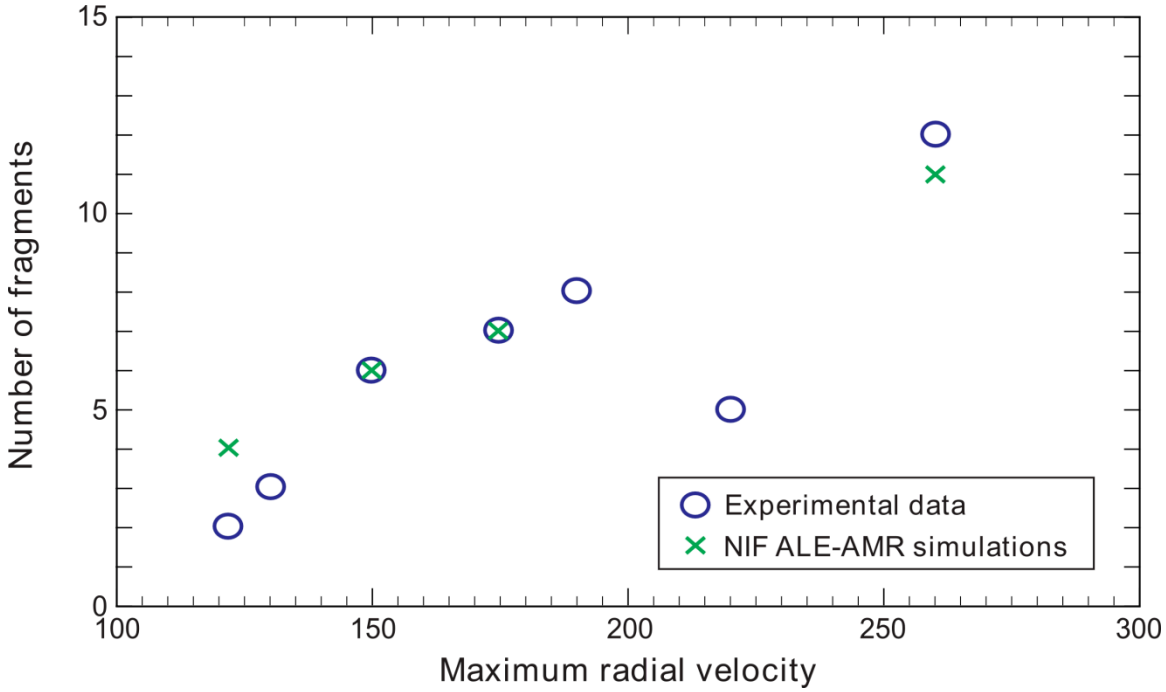

Figure 3: Comparison of the fragmentation results from the Altynova experiments [17] and the NIF ALE-AMR simulations. In the experiment, higher energies discharged across the solenoid drive the rings to higher velocities and higher fragment counts.

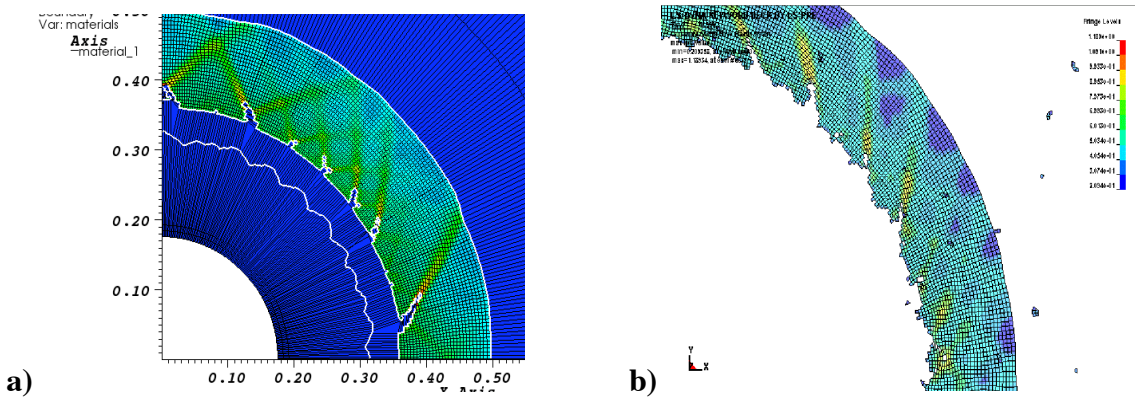

Figure 4: A code-to-code comparison of pressure driven ring fracture between NIF ALE-AMR (a) and LS-DYNA (b). These images at 15μs show similar plastic strain occuring and the rings forming similar fragment sizes.

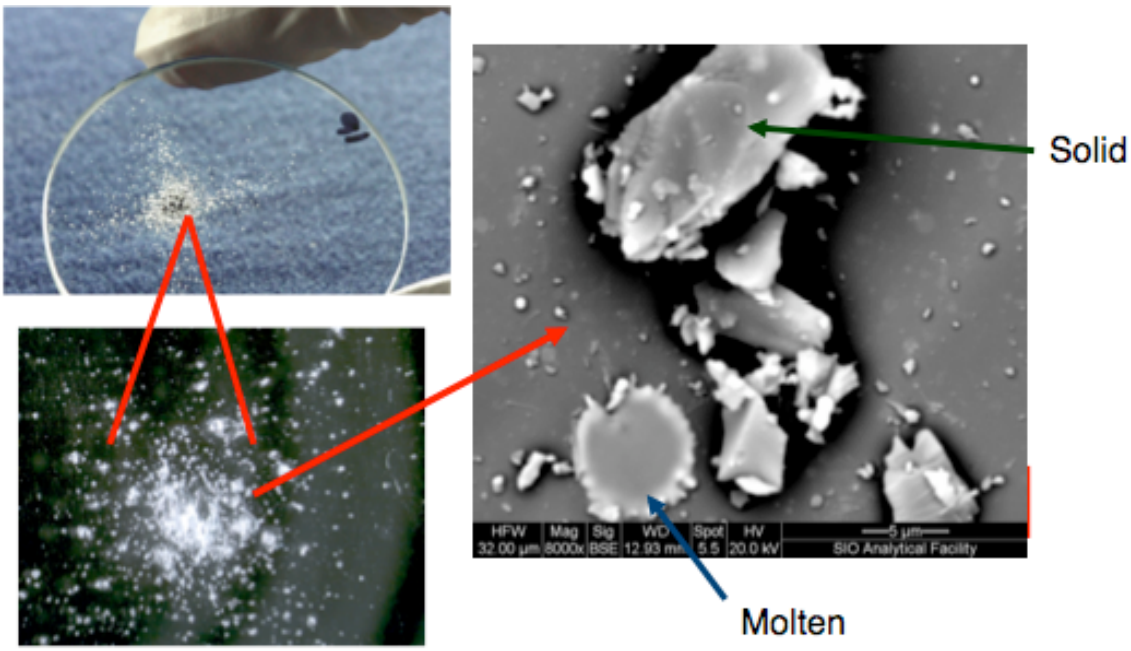

Figure 5: Shrapnel captured on glass plates from Janus laser-driven spall experiments show evidence of both solid and molten fragments.

.

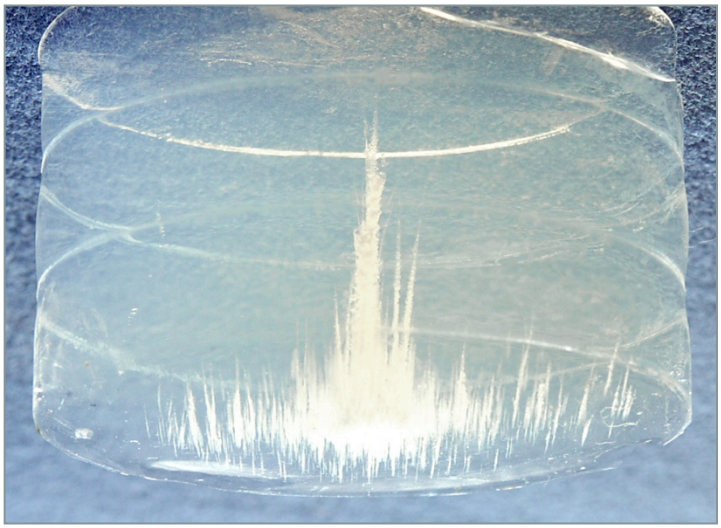

Figure 6: Penetration of shrapnel fragments in aerogel sample can be used to determine velocity of fragments.

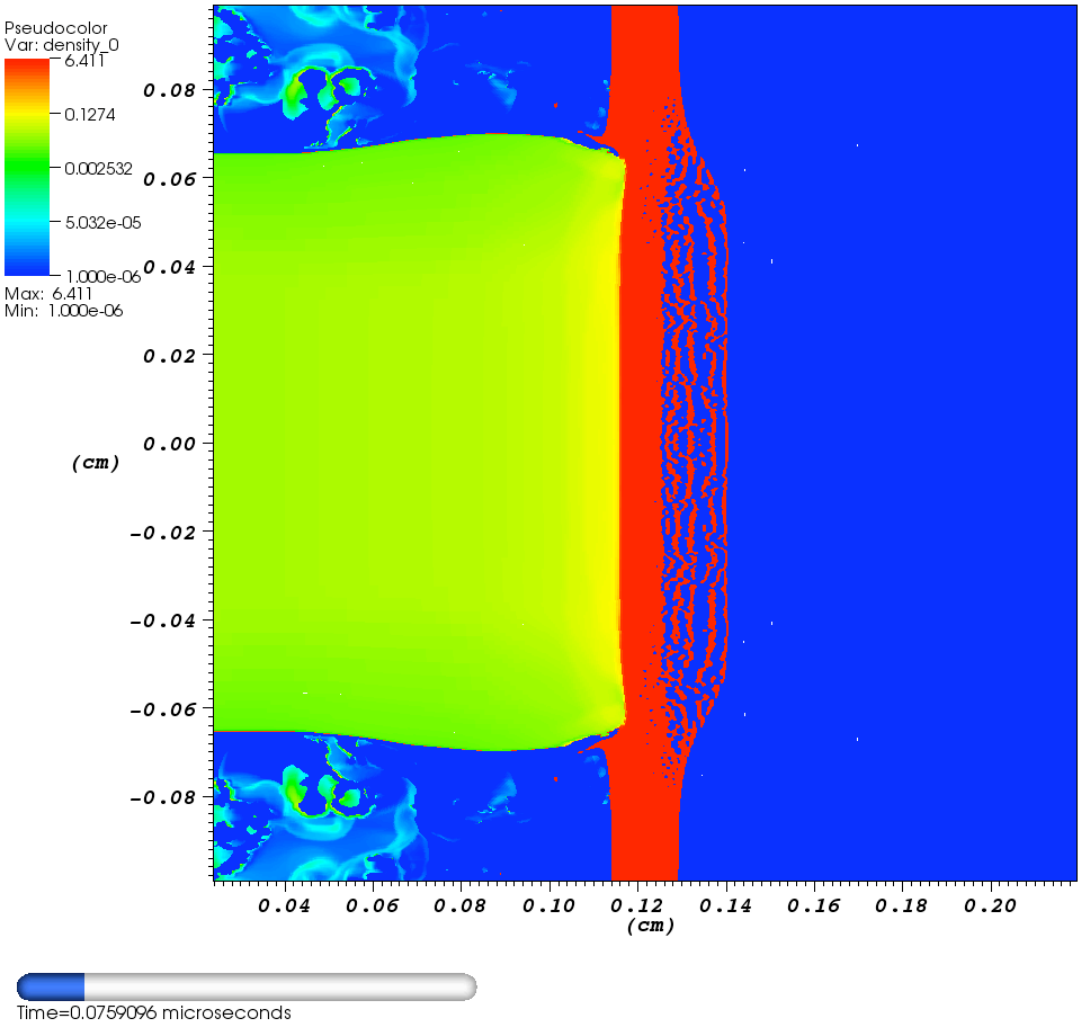

Figure 7: NIF ALE-AMR simulation showing fragmentation off the back side of a Vanadium foil energized on the left side (note plasma plume in yellow-green) for comparison with Janus experiments.

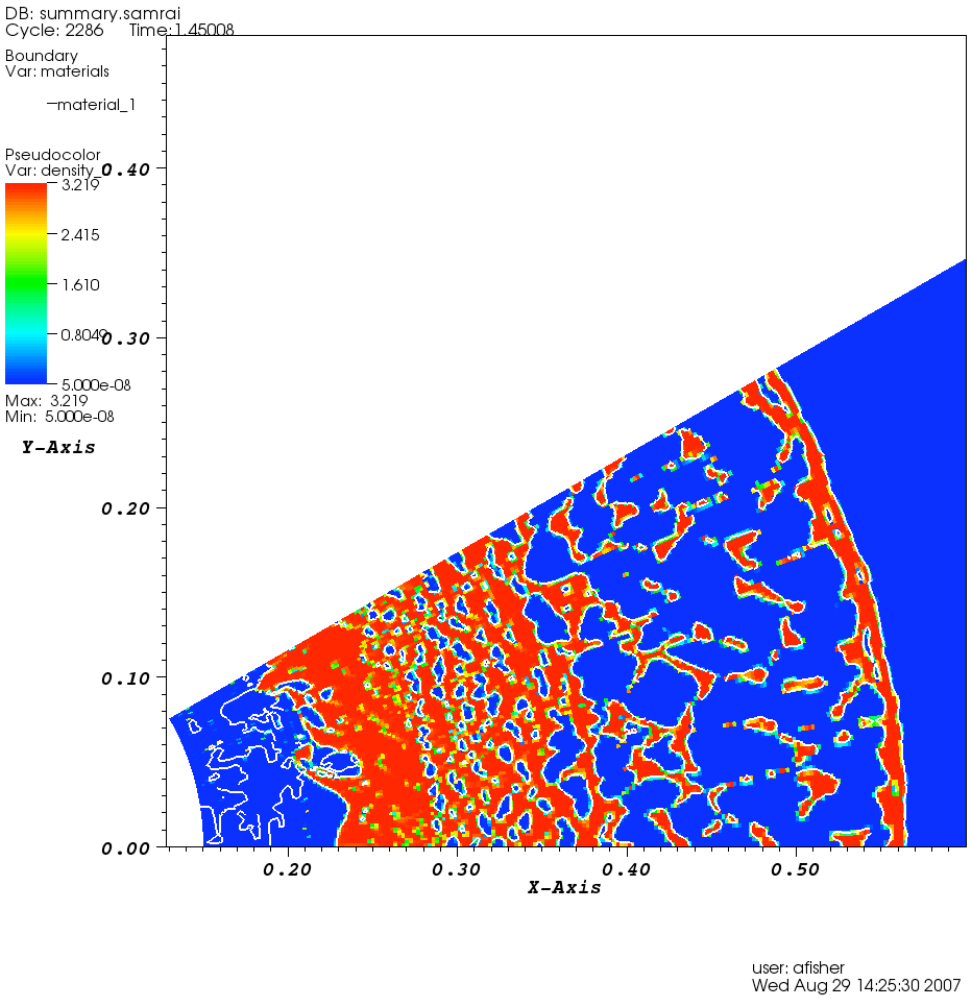

Figure 8: Simulation results for the Si cooling ring at 1.45μs. The brittle properties of Si cause the ring to fragment into many small pieces.

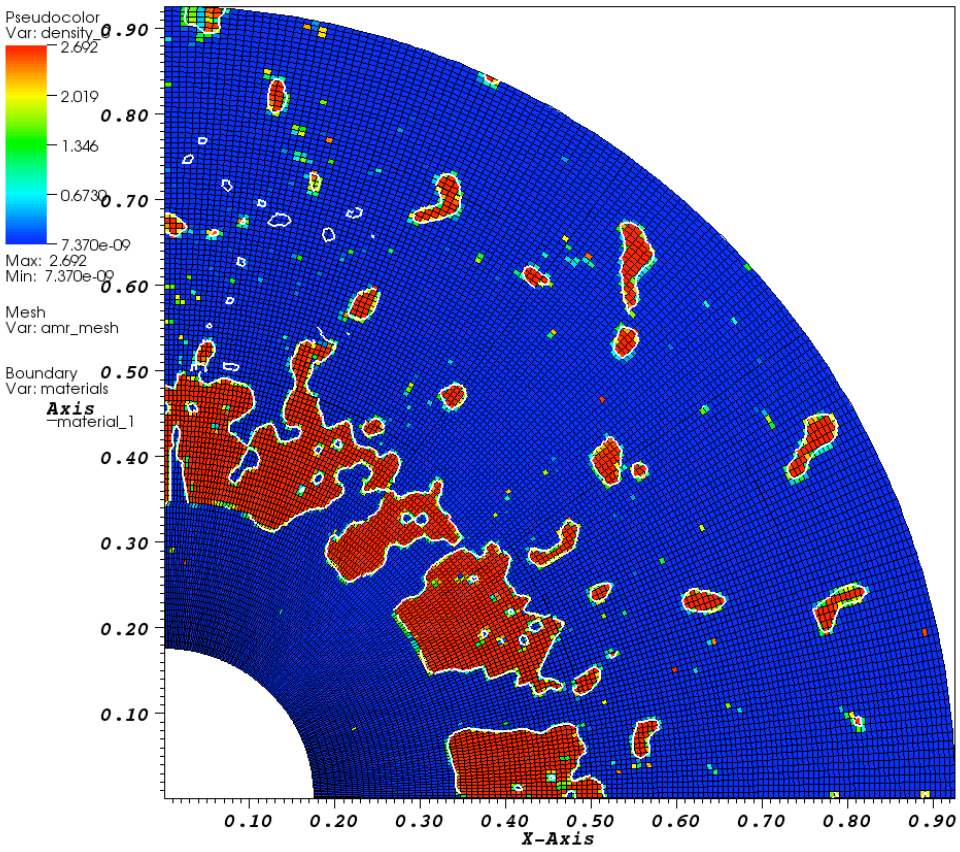

Figure 9: Simulation results for the Al cooling ring at 14μs. The ductile properties of Al cause the ring to fragment into larger pieces than the Si cooling ring.

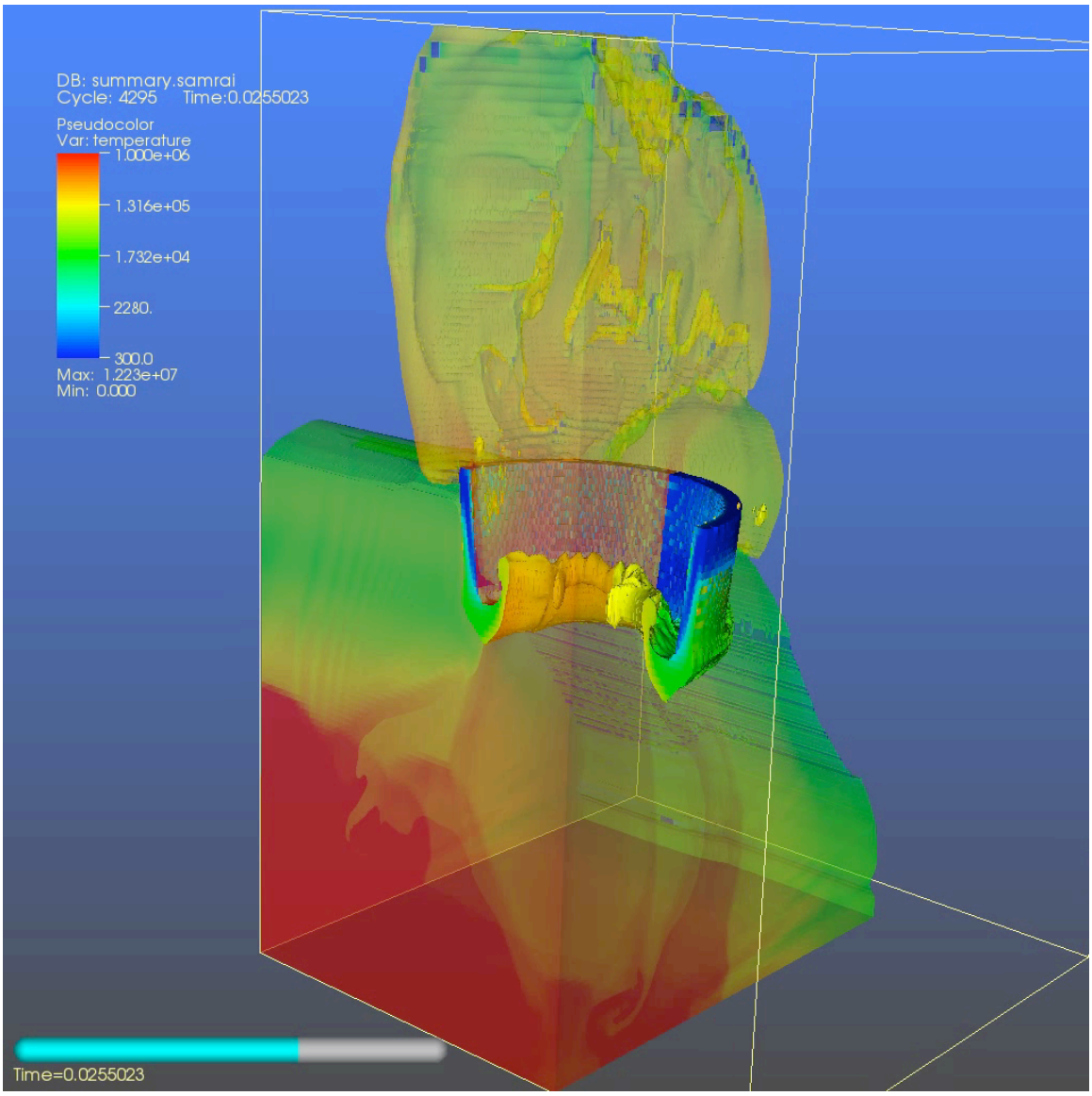

Figure 10: NIF ALE-AMR temperature profile results of a shock timing diagnostic keyhole target . Viewing of the outer cone is facilitated by the semi-transparent rendering of the vaporized material of the hohlraum and inner cone. This simulation predicts that the outer cone will melt or vaporize rather than being accelerated intact.